A Self-Consistent Model For Directional Dependence Of Crack Growth

Xi Zhang[1], Rob Jeffrey[1] and Yiu-Wing Mai[2]
[1]CSIRO Petroleum, PO Box 3000, Glen Waverley, Victoria 3150, Australia
[2]Centre for Advanced Materials Technology (CAMT), School of Aerospace, Mechanical and Mechatronic Engineering J07, University of Sydney, Sydney, NSW 2006, Australia

ABSTRACT

Fracture growth is considered as the competition between cleavage and dislocation self-organization in elastic-plastic solids. A self-consistent model is proposed to bridge the responses at relevant length scales, an elastic enclave in the immediate vicinity of crack tip, an array of disclination dipoles and macroscopic plastic deformation. The directional dependence of crack growth is studied. In the continuum limit, the flow stress is expressed by a spatial coupling in terms of a second-order gradient of the rotation strength of disclination dipoles. An estimate of the core size and the crack-tip shielding ratio is given by identification of the macroscopic plastic fields, the elastic field and the constitutive flow stress from the micromechanics consideration, on the boundary of elastic core. Strong dependence of apparent fracture toughness on the intrinsic surface energy and the ductile-to-brittle transition are examined.
Key words: Crack growth, direction, disclination dipole, kink, core size, shielding ratio

INTRODUCTION

Crack growth operates on different length scales due to high stress and strain gradients and continuum models allowing for finite scale effects are needed to account for multiscale mechanisms. Most studies on ductile versus brittle fracture behaviours focused on the competition of dislocation emission from the crack tip and cleavage fracture [Kelly et al., 1967; Rice and Thomson, 1974; Zhang, 1990; Fischer and Beltz, 2001]. However, other energy dissipation mechanisms such as preexisting mobile dislocations may play an important role. Creation and motion of dislocations near the crack tip may give rise to collective response in increasing the ductility of the materials [Orowan, 1945; Irwin, 1948]. Usually, plastic deformation on different length scales is interconnected and exceeds the free energy of the newly created surface by orders of magnitude. Fracture mechanics theories proceed from the idea of the existence of a close relation between length scales and the crack size so that some distributions and types of flaws may shield, and others anti-shield, the crack tip in terms of changing critical stress intensity factors [Zhang, 1990] or considering energy dissipation mechanisms [Kysar, 2003].

There exists a microdefect-free ligament directly ahead of the crack tip at the atomic scale level. A dislocation-free zone ahead of the crack tip has been detected in single crystals of stainless steels, copper and aluminium subjected to tension and cyclic loading [Ohr et al., 1982]. Outside this zone, a massive dislocation activity can take place on the mesoscopic level by stress-assisted cooperative dislocation movement. These cooperative effects manifest qualitatively new properties by forming a system of disclinations when their total number exceeds a certain value. There is a need to examine the effect of plastic dissipation on material fracture.

Several proposals have been made to define the characteristic length for size effects. These include (i) the Burgers vector [Lipkin et al, 1996], (ii) the spacing of barrier to dislocation motion [Beltz et al., 1996], (iii) the spacing of Frank-Read sources [Kysar, 2003], $L_c = \rho^{-1/2}$ in which ρ is the dislocation density, and (iv) a plastic zone with many low-mobility dislocations at a radius of the order $10^{3-4}\,b$ has predicted [Suo et al., 1993]. The cooperative effect of high-density dislocations may behave as a disclination dipole or a superdislocation [Romanov and Vladimirov, 1992]. Especially, plastic deformation can be localized into a kink or misorientational band emitted from

the crack tip. The disclination dipoles distribute uniformly inside the misorientation band, but with different rotation strength corresponding to stress and strain gradients. The dipole arm proportional to the width of the kink band, is of the order of thousands of the Burger's vector, in the order of 0.1-1 μm. These disclination dipoles also interact with each other so as to minimize the potential energy, and a continuum limit exists. In this paper, we will focus on the understanding of the effect of disclination plasticity on the crack growth in some preferred directions.

DISCLINATION-BASED CRACK-TIP PLASTICITY

For a geometrical description of disclinations, we start with a uniform hollow cylinder having a radial cut, the typical wedge disclination of Somigliana type. By turning the faces of the cut and subsequently sticking them together, one can find a disclination related to the rotation of non-deformed faces of the cuts by an angle ω, the Frank vector, about the fixed axis.

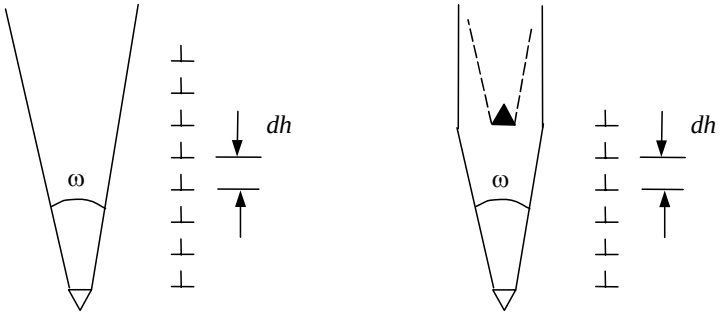

Figure 1: Dislocation description of wedge disclinations and their dipoles

There is a relationship between disclinations and dislocations. A straight wedge disclination can be represented in terms of an array of dislocations, as shown in Fig. 1. An disclination with the power ω is identical to a semi-infinite wall of edge dislocation having linear density ρ:

$$\rho = 1/dh = 2\tan(\omega/2)/db = \omega/db \qquad (1)$$

in which dh is the spacing of dislocations.

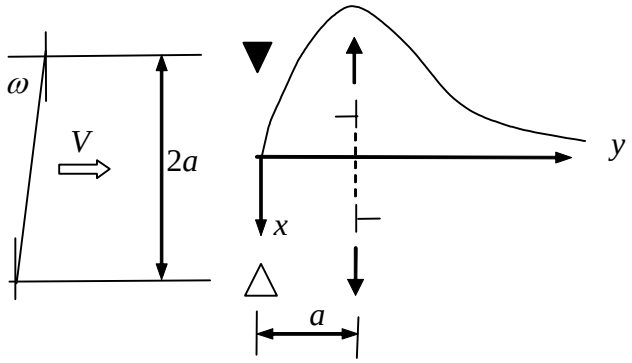

Figure 2: Disclination hardening mechanism. A steady moving disclination dipole motion is related to redistribution of dislocations in front of the dipole.

The semi-infinite dislocation wall seems to be impossible in crystalline solids because it needs adequate energy. But, most disclinations with opposite sign can exist in the form of a wall cut off from two sides, as a disclination dipole illustrated in Fig. 1. It can be found in Romanov and Vladimirov (1992) that the energy for the formation of disclination dipoles is nearly the same as a single edge dislocation. To calculate the flow stress in the presence of disclinations, let us consider the motion of a disclination dipole that interacts with gliding dislocation loops in front of the moving disclination dipole at a steady speed *V*, as illustrated in Fig. 2. The central plane of the

microrotation band suffers the maximum shear stress that is equal to, [Romanov and Vladimirov, 1992]:

$$\sigma_{xy} = D\omega g(y) + \tau_e \qquad (2)$$

in which $D = G/2\pi(1-\nu)$; $g(y) = ya/(y^2 + a^2)$; τ_e refers to the critical shear stress above which the disclination dipole nucleation occurs and is of the form $\tau_e = \sigma_*(1 - T/T_c)$, in which T and T_c are the temperature and the reference temperature respectively, and σ_* is the reference stress for a special material.

It follows from (2) that the maximum flow stress is:

$$\sigma_{flow} = \tau_e + 0.5D\omega \qquad (3)$$

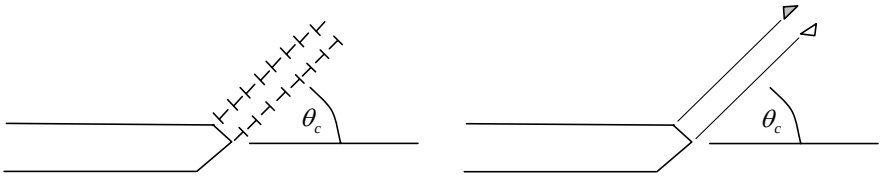

Figure 3: Generation of a micro-orientational band at an angle θ_c to the crack line. The arrays of dislocations can be represented by disclination dipole motion at θ_c.

Materials ahead of a crack tip experience a non-uniform distribution of stresses. An example of a relaxation process, in this case, twinning, is shown in Fig. 3 with a periodic array of disclination dipoles to form a kink band. The kink band has been modelled [Flouriot et al., 2003] in a single crystal CT specimen using finite element method. It can be simplified by the disclination dipoles, as shown in Fig. 3, which move quasi-statically in the direction of θ_c to the crack line. The dipole motion reduces the stress levels directly in front of the crack tip and create a local overstress at a certain distance. The asymmetric crack geometry is expected in the presence of a preferred direction of mobile dislocations, as shown in Fig. 3.

We now express the coupling term inside the band by a discrete form that takes into account the interaction of a dipole with its two nearest neighbours. It is assumed that the disclination power varies along the thickness of the kind band and the effective disclination arm is also equal to 2*a*. So, the flow stress in elastic medium is [Romanov and Vladimirov, 1992]:

$$\sigma_{flow} - \tau_e = -2Da^2\nabla^2\omega \qquad (4)$$

THE MODEL

We shall build our qualitative model on the framework previously proposed for cleavage in the presence of mobile dislocations[Suo et al., 1993; Beltz et al., 1993; and Lipkin et al., 1996]. Fig. 4 shows schematically the physical basis for our analyses of initiation of cleavage fracture under small scale yielding condition. The crack tip is located in a single grain and the material surrounding the crack is allowed to plastically deform with strain hardening prior to cleavage. There exists a core region with radius R_c in which the material behaves as an elastic medium. The continuum assumption of disclination dipoles can be justified, as the radius is greater than R_c.

In the region outside the core, a power-law elastic-plastic constitutive law is valid. The asymptotic stress field for homogeneous deformation at small distance, *r*, from the crack tip can be taken as the modified singular HRR field [O'Dowd and Shih, 1991]. The effective stress $\bar{\sigma}$ in this so-called J-Q field has the form:

$$\overline{\sigma} = \sigma_0 (\frac{\xi}{\beta I_n} \frac{K_{I\infty}^2}{r\sigma_0^2})^{1/(1+n)} \overline{\sigma}_n + Q\sigma_0 \tag{5}$$

in which Q represents the crack-tip constraint; $K_{I\infty}$ is the applied stress intensity factor that characterizes the elastic field well beyond the plastic zone, and the measured energy release rate $G_\infty = \xi K_{I\infty}^2 / E$. σ_0 is the yield strength. The parameter ξ represents the state of loading mode, 1 for plane stress and $1-\nu^2$ for plane strain. n and β are material constants in power-law plasticity. $\overline{\sigma}_n$ is a weak function of θ. I_n is a wake function of the work-hardening exponents.

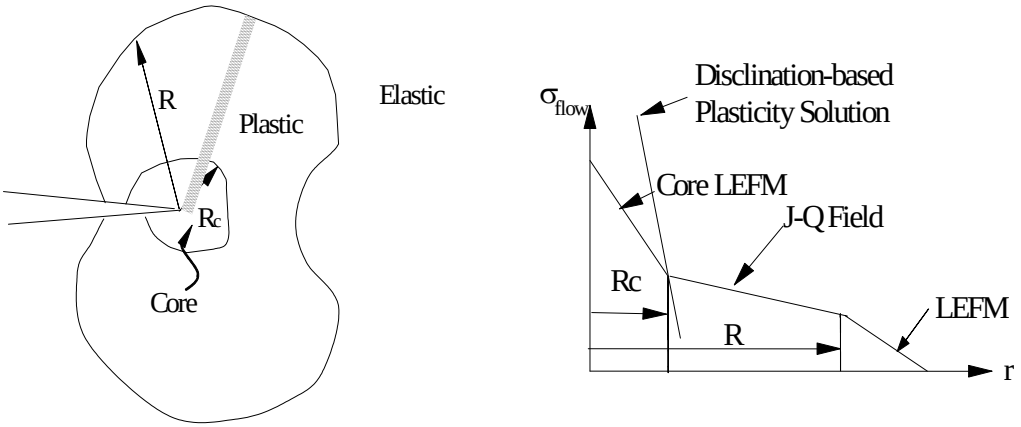

Figure 4: Physical sources for cleavage fracture in the presence of plastic flow (a) microrotational bands, plastic zone and elastic core; (b) idealized stress distribution at θ_c ahead of the tip.

In the core region, the stress field inside the core region takes the form of an elastic singularity described by a crack-tip stress intensity factor $K_{tip} = \sqrt{EG_{tip}/\xi}$. The effective stress inside it can be approximately evaluated from the standard solutions in LEFM:

$$\overline{\sigma} = \lambda \frac{K_{tip}}{\sqrt{r}} \tag{6}$$

in which the angular factor $4\pi\lambda^2 = (8\nu^2 - 8\nu + 5 - 3\cos\theta)\cos^2(\theta/2)$ for plane strain Mode I cracks.

Furthermore, the second gradient of the rotation ω is expressed as follows:

$$\nabla^2 \omega = \varepsilon_{12,11} - \varepsilon_{11,12} + \varepsilon_{22,12} - \varepsilon_{21,22} \tag{7}$$

Combining (4) and (7), we can obtain the expression for the flow stress as:

$$\sigma_{flow} = \tau_e - 2\beta D\varepsilon_0 (\frac{a}{r})^2 (\frac{\xi}{\beta I_n} \frac{K_{I\infty}^2}{r\sigma_0^2})^{n/(1+n)} \tilde{\Delta}(n,\theta) \tag{8}$$

It is expected that the maximum radius of the core occurs along the angle θ_c where the value of $\tilde{\Delta}$ reach the maximum. Enforcing continuity of effective stress on the core boundary along the fixed direction, $\theta = \theta_c$, we can equate the equation (5), (6) and (8) to calculate the radius of the elastic core R and the ratio G_∞ / G_{tip}. Thus we can obtain:

$$\frac{\lambda\sqrt{\delta}}{\sqrt{\xi}} (\frac{R}{a})^{-0.5} = \frac{\tau_e}{\sigma_0} + a_1 [\frac{\lambda\sqrt{\delta}}{\sqrt{\xi}} (\frac{R}{a})^{-0.5} - Q]^n (\frac{R}{a})^{-2} \tag{9}$$

$$\chi = \beta I_n (\frac{R}{a}) \{ [\frac{\lambda\sqrt{\delta}}{\sqrt{\xi}} (\frac{R}{a})^{-0.5} - Q] / \overline{\sigma}_n \}^{n+1} \tag{10}$$

in which $\delta = \frac{EG_{tip}}{\sigma_0^2 a}$; $\chi = \frac{EG_\infty}{\sigma_0^2 a}$ and $a_1 = \frac{2\beta D}{E} \left|\tilde{\Delta}\right| / (\overline{\sigma}_n)^n$.

AN EXAMPLE

Consider the semi-infinite crack problems in an infinite medium. Table 1 gives the material constants required for solving Eqs. (9) and (10). Figure 5 shows the variations of the core size and the shielding ratio in the case of Q=0 and σ_*=0. It can be seen that both the core size and the shielding ratio depend much on the work-hardening exponents and the intrinsic fracture toughness G_{tip}. For the normalized quantity δ up to 10^4, $G_{tip}/\sigma_0 b$<300 [Beltz et al., 1996] because E/σ_0~1000 and *a*/*b*=20. An increase in *n* and G_{tip} gives rise to an increase in the core size and G_∞, although a reverse trend is found for *n*=2.5 and δ is less than 500. A slight variation in G_{tip} leads to a dramatic change in R_c/a and G_∞/G_{tip}, especially for low hardening materials. The larger the value of *n* is, the more important the shielding ratio. This trend is in good agreement with existing results [Suo et al., 1993; and Beltz et al., 1996]. The shielding ratio can reach 10^4 for *n*=10 and 10^3 for *n*=5, the same order as those using FEM technique [Suo et al., 1993; Beltz et al., 1996]. In addition, the core size ranges from several to 100 times of the dipole arm. As *a* ranges from several to 50*b*, the core region would have the order of several hundreds of the lattice constants, that is, on the order of 0.1-1μm, in good agreement with the predictions [Lipton et al., 1996; Beltz et al., 1996].

Table 1: Selected values of HRR parameters under plane strain condition

n	θ_c	$\overline{\sigma}_n$	I_n	$\tilde{\Delta}$
10.0	0.648	0.78	4.5	-1.9385
5.0	0.517	0.61	5.0	-1.6542
2.5	0.247	0.20	5.7	-1.5533

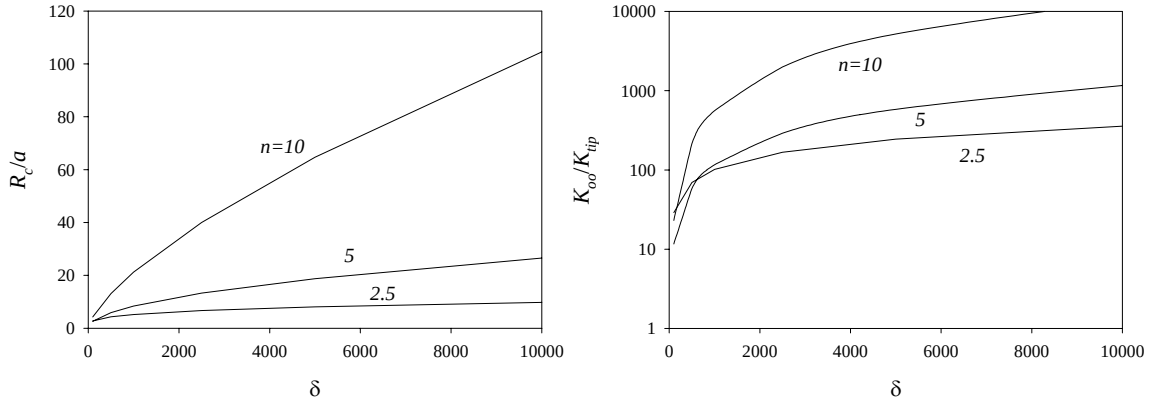

Figure 5: (a) Core size versus the intrinsic toughness and (b) Crack-tip shielding ratio versus the intrinsic toughness for various *n* at Q=0 and $T = T_c$.

The Ductile-Brittle transition is reported in Fig. 6 through the dependence of fracture toughness on temperature, under the conditions σ_*/σ_0=1, 1.5, 2 and δ=500. The sharp drop of G_∞/G_{tip} at low temperature implies the occurrence of transition. It is interesting to note that the dislocation-free zone increase with decreasing temperature. Therefore, the plastic deformation is retarded by the expansion of the dislocation-free zone. Lower fracture toughness is expected in this case.

Figure 7 displays the dependence of R_c/a and G_∞/G_{tip} on the crack-tip constraint. It can be seen that the fracture toughness is enhanced by the loss of crack-tip constraint. This feature is more pronounced when *n*=10. It reveals that the constraint effect is more important for low work-hardening materials.

Moreover, the kink band is located at an angle θ_c to the crack line, rather than directly ahead of the crack tip in the previous model [Lipkin et al., 1996]. The strain localization in these kink bands can yield a shielding effect on the crack tip field. Sometimes, it leads to the blunting of the crack tip. This toughening mechanism is well known [Romanov and Vladimirov, 1992].

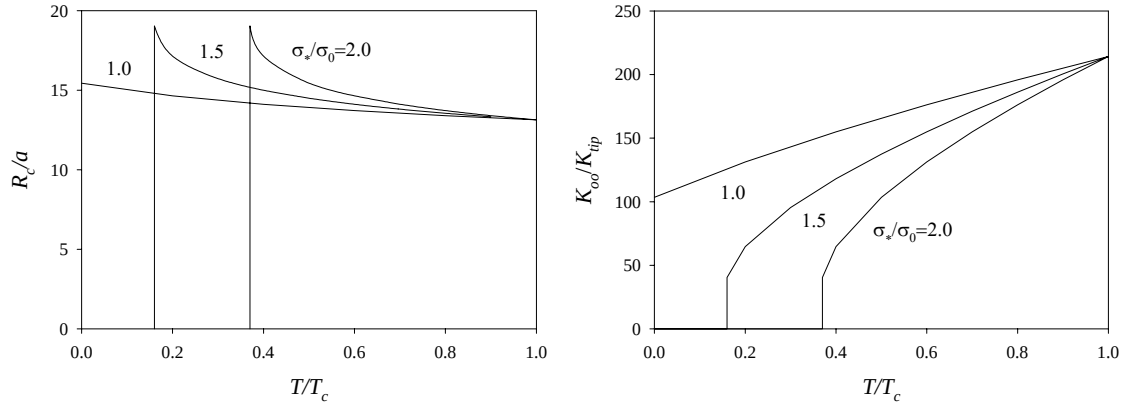

Figure 6: Dependence of (a) the core size and (b) the shielding ratio on temperature for varying values of the ratio σ_* / σ_0 at n=10, Q=0 and δ=500.

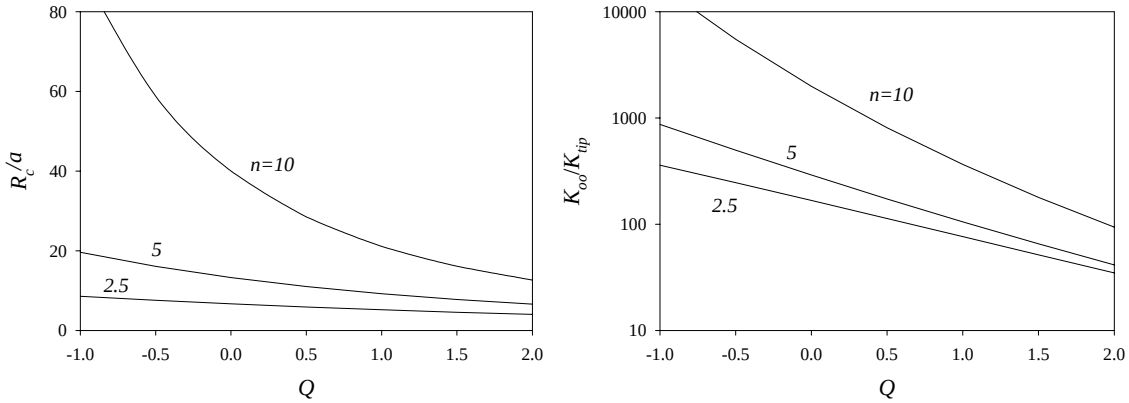

Figure 7: Dependence of (a) core size and (b) shielding ratio on crack-tip constraint for various values of n at $T = T_c$ and δ=2500.

CONCLUSIONS

In this paper, an effort was made to examine the directional dependence of crack growth in the presence of intense plastic deformation. The mobile dislocations can evolve into a kink band to shield the crack tip. A continuum model based on the disclination mechanism is proposed to account for relaxation of stress levels ahead of the crack tip. However, stress relaxation may be hindered by the cleavage process. A self-consistent model is presented in this paper to account for the competition between energy dissipation in terms of disclinations and the cleavage fracture in homogeneous materials. The elastic core size and the crack-tip shielding ratio are obtained for crack growth orientated in one direction with maximum absolute value of the second-order gradient of rotation. For low hardening materials, the core size is larger in order than the dislocation spacing. In addition, strong dependence of apparent fracture toughness on the intrinsic surface energy and the ductile-to-brittle transition caused by both thermal effect and crack–tip constraint are found.

REFFERENCES

Beltz, G. E., Rice, J. R., Shih, C. F. and Xia, L. A self-consistent model for cleavage in the presence of plastic flow, *Acta Mater*. **44**, 3943(1996).

Fischer, L.L. and Beltz, G. E. The effect of crack blunting on the competition between dislocation nucleation

and cleavage, *J. Mech. Phys. Solids* **49**, 635(2001).
Flouriot, S, Forest, S., Cailletaud, G., Koster, A., Remy, L., Burgardt, B., Gros, V., Mosset, S. and Delautre, J. Strain localization at the crack tip in single crystal CT specimens under monotonous loading: 3D Finite Element analyses and application to nickel-base superalloys, *Int. J. Fracture* **124**, 43(2003).
Irwin, G. R. Fracture mechanics, In: Fracturing of Metals, Eds. Jonassen, F. et al., American Society of Metals, Cleveland, 147(1948).
Kelly, A., Tyson W., and Cottrell, A. Ductile and brittle crystals, *Phil Mag* 15 567(1967).
Kysar, J. W. Energy dissipation mechanisms in ductile fracture, *J. Mech. Phys. Solids* **51**, 795(2003)
Lipkin, D. M., Clark, D. R. and Beltz, G. E. A strain-gradient model of cleavage fracture in plastically deforming materials, *Acta Mater*. **44,** 4051(1996).
O'Dowd, N. P., and Shih, C. F. Family of crack-tip fields characterized by a triaxility parameter, I Structure of fields, *J. Mech. Phys. Solids* **39**, 989(1991).
Ohr S. M., Horton, J. A., and Chung, S. J. (1982) Direct observation of crack tip dislocation behavior during tensile and cyclic deformation, Defects, Fracture and Fatigue, G. C. Sih and J. W. Provan, eds., Martinus Nijhoff Publishers, the Netherlands, 3-15.
Orowan, E. (1945) Notch brittleness and the strength of metals, Proceedings of the Society of Engineers and Shipbuilders, Paper No. 1063, Scotland.
Rice, J. R. and Thomson, R. Ductile versus Brittle behavior of crystals, *Phil. Mag*. **29**, 73(1974).
Romanov, A. E. and Vladimirov, V. I. (1992) Disclinations in crystalline solids, chapter 47 in Dislocations in Solids, No. 9, F. R. N. Nabarro ed., Elsvise Science Publishers, 191.
Suo, Z., Shih, C. F. and Beltz, G. E. A theory for cleavage cracking in the presence of plastic flow, *Acta Metall. Mater*. **41**,1551(1993).
Zhang, T.-Y. Computer Simulation of Semibrittle Fracture, *Zeitschrift für Metallkunde*, **81** 63(1990).